

VELOCITY PROFILES AND SCOUR DEPTH MEASUREMENTS AROUND BRIDGE PIERS

by

Vincenza C. Santoro¹, Pierre Y. Julien², Everett V. Richardson³
and Steven R. Abt⁴

ABSTRACT

Local scour around a model of the Schoharie bridge pier was experimentally investigated in the laboratory. The tests simply focused on the effects of the angle of attack and flow velocity on the maximum depth of scour. Clear water scour conditions prevailed, i.e. the shear stress at the bottom in the upstream flow is always less than the critical value for beginning of sediment motion. The experimental results show that the effect of the angle of attack is related to the undisturbed flow Froude number. In particular, the ratio of the measured scour depths for skewed and aligned piers decreases with increasing Froude number. Velocity is found to have an important influence on scour depth.

INTRODUCTION

The 1987 bridge failure on the Schoharie Creek in the State of New York claimed ten lives and required considerable effort to rebuild the structure. The bridge collapse has been attributed to the scouring action of the flow around its piers. The risk of bridge failure due to pier scour and the design of appropriate countermeasures remain serious concerns for thousands of bridges in the United States and abroad. The past 50 years of research provided basic understanding of the physical mechanism of local scour. Nevertheless, the quantitative dependence of the scour depth on the scouring parameters justifies further investigations because existing scour equations are not yet fully reliable.

¹ Asst. Prof. of Civil Engineering, Istituto di Idraulica Idrologia e Gestione delle Acque, Universita di Catania, V. le A. Doria 6, 95125 Catania, Italy.

² Assoc. Prof. of Civil Engineering, Engineering Research Center, Colorado State University, Fort Collins, CO 80523, 303/491-8450.

³ Prof. of Civil Engineering, Engineering Research Center, Colorado State University, Fort Collins, CO 80523, 303/491-8582.

⁴ Prof. of Civil Engineering & Director of the Hydraulics Laboratory, Engineering Research Center, Colorado State University, Fort Collins, CO 80523, 303/491-8203.

A series of experiments was conducted at Colorado State University using a laboratory model of one of the Schoharie Creek bridge piers. The main objective was to investigate pier scour under the effects of two variables: angle of attack and mean flow velocity. Two sets of runs, one with the pier aligned with the flow and one with the pier angled at 10° with respect to the main flow direction were completed. Within each set of runs the upstream velocity was maintained below the critical conditions of motion of the bed material, thus clear water scour conditions prevailed during the experiments. Scour depth, change in water surface elevation, time-average point velocity and maximum velocity fluctuations were measured along six cross-sections near the pier.

EXPERIMENTAL SETUP AND PROCEDURE

The experiments were conducted in a 61 m x 2.4 m x 1.2 m recirculating laboratory flume at the Engineering Research Center. A large scale model, scale 1:15, of the Schoharie Creek bridge pier is shown in Fig. 1. The footing has a rectangular shape, wider and longer than the pier itself, which is well rounded on both ends. Metal pieces fixed the model pier to the flume sidewalls. Pea-size gravel ($D_{50} = 3.3$ mm) covered the flume bed up to the top of the foundation footing. Rails on the top of each flume sidewall supported a motorized carriage holding a point gage, a depth measuring device and the current meter probe used for velocity measurements. From a total of six tests, the first three showed the pier aligned with the flow, the remaining three showed the pier skewed at an angle α of 10° between the pier axis and the main flow direction. The discharge and slope were controlled to maintain average velocities of 0.3, 0.6 and 0.9 m/s while keeping the flow depth constant at $y_1 = 0.3$ m for each run. The test conditions are summarized in Table 1. The downstream conditions were controlled by a tail gate. With the study reach located 30 m upstream of the tailgate, steady uniform flow conditions prevailed in the study reach without the pier. Each run was allowed sufficient time, at least 8 hours, to simulate conditions approaching the maximum expected scour.

Reference nets in Figs. 2 and 3 show the location of each measuring vertical. In the case of the aligned pier, measurements were taken on only half the flow field after checking the symmetry in velocity profiles on each side of the pier. At least five velocity measurements were taken on each vertical, except where deposits significantly reduced the flow depth. When the erosive action would allow it, measurements were also taken below the "zero reference" (the elevation of the undisturbed bed).

Velocity measurements were taken using a Marsh-McBirney 2D electromagnetic current meter. Average values and maximum fluctuations of the two velocity components parallel and perpendicular (in a plane parallel to the bottom of the flume) to the main flow direction were recorded. The current meter was connected to an HP 3468 Multimeter connected to an HP 82162A thermal printer and to an HP 71 calculator in an IL loop. Over a period of 30 seconds, 57 measurements were read, stored and averaged for each probe position and each flow direction. Changes in the bed elevation and water surface elevation profiles were also compiled from these measurements by Santoro (1989).

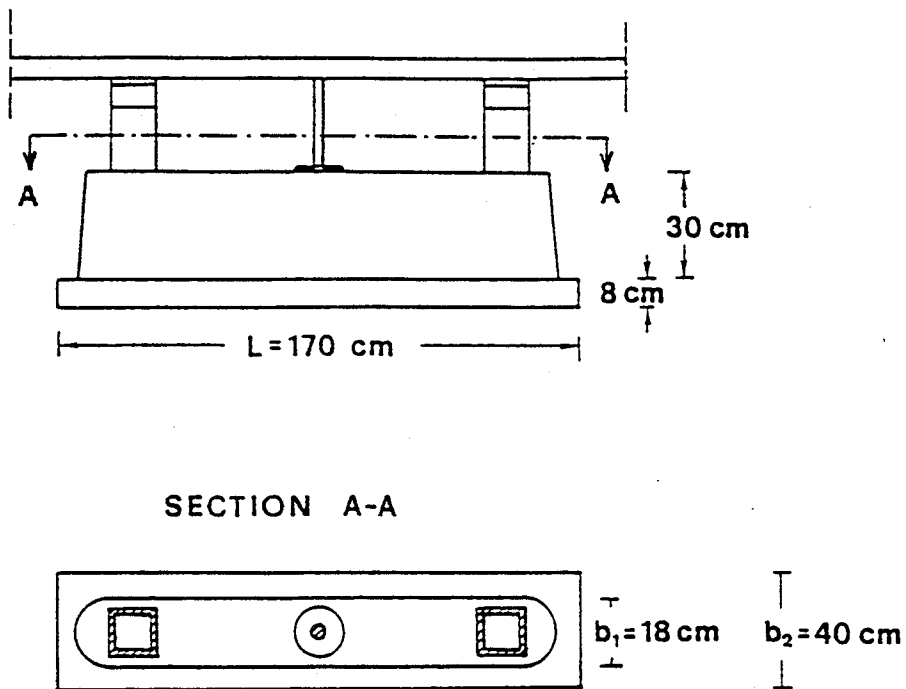


Figure 1. Geometric characteristics of the Schoharie bridge pier model.

Table 1. Summary of tests conditions.

Run number	Upstream flow depth y_1 [m]	Upstream flow velocity V [m/s]	Discharge Q [m ³ /s]	Slope S [%]	Froude number Fr	Pier Angle α
1	0.3	0.3	0.223	0.014	0.176	0°
2	0.3	0.6	0.447	0.055	0.352	0°
3	0.3	0.9	0.670	0.123	0.529	0°
4	0.3	0.3	0.223	0.014	0.176	10°
5	0.3	0.6	0.447	0.055	0.352	10°
6	0.3	0.9	0.670	0.123	0.529	10°

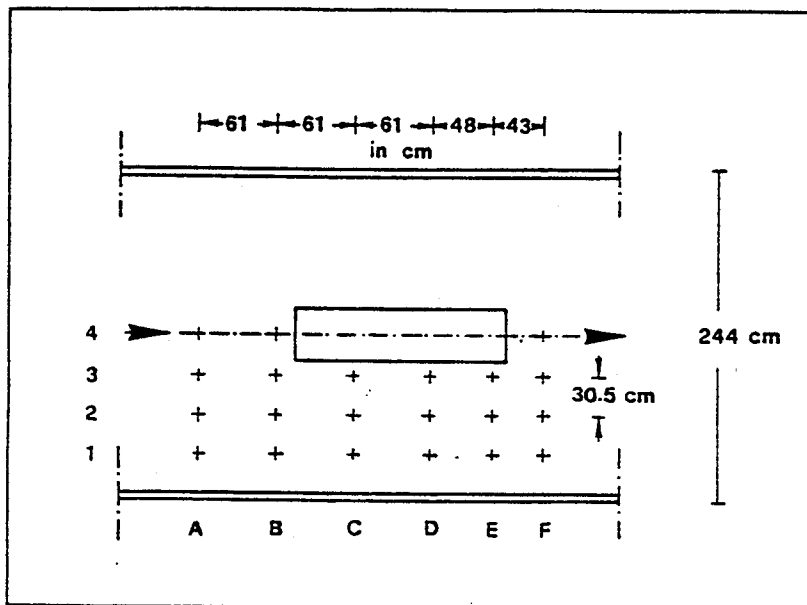


Figure 2. Reference net for aligned pier ($\alpha = 0^\circ$).

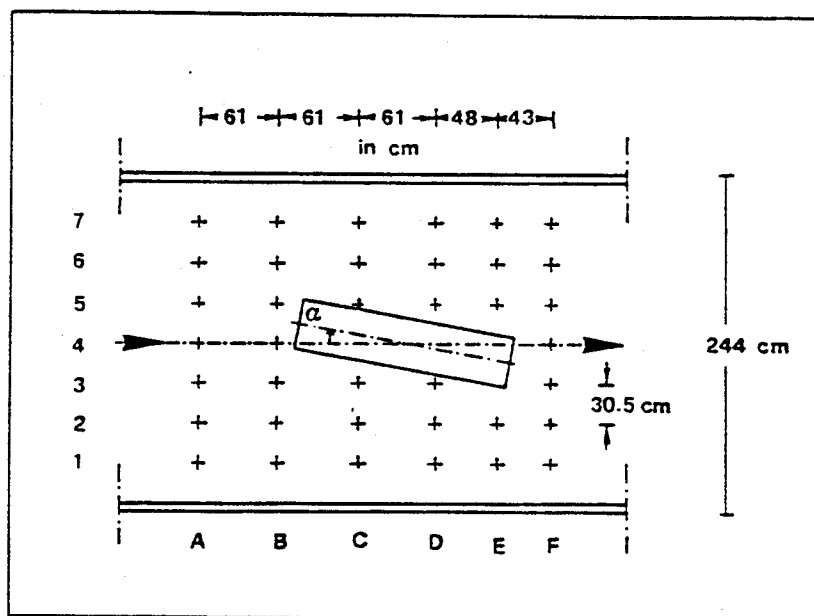


Figure 3. Reference net for angled pier ($\alpha = 10^\circ$).

RESULTS

Flow Patterns Around the Pier

The downstream velocity distribution was obtained from the measurements at each cross-section and at planes parallel to the flume bed. The flow is slowed down in the central area upstream of the pier, this effect is accentuated for the angled pier. Figure 4 shows the results of the measured velocity distribution at cross-section C from Run 4 for the angled pier. The velocity is maximum on the side the pier is skewed toward, and the maximum velocity is found at an elevation ranging between 0.4 and 0.7 of the undisturbed flow depth y_1 . The ratio of the maximum measured velocity to the undisturbed flow velocity is 1.4 for the aligned pier and 1.6 for the angled pier.

Lower velocity is measured in the wake of the pier and asymmetric profiles result for the angled pier. Figure 5 shows a planview of the dimensionless velocity distribution in a section parallel to the bottom of the flume set at an elevation corresponding to 0.4 of the undisturbed flow depth y_1 . The overall flow pattern is well described in that maximum velocities are found on the narrow sides of the skewed pier. The number of verticals, however, precludes any detailed analysis of the flow near the pier and along the sidewalls.

Discharge measurements from the orifice inserted in the recirculating pipeline compared favorably with the calculated discharge from the integration of the velocity distribution over the cross-section.

Total Scour Around the Pier

The total scour around the pier combines the effects of two causes: contraction scour due to the higher velocity in the reduced cross-section area near the pier, and local scour due to the horseshoe vortex around the base of the pier. Qualitative and comparative information can be drawn from the photographs and measurements of the flume bed surface at the end of each run.

Under low flow velocities, the extent of scour is relatively limited downstream of the pier. Only the front part of the pier was exposed. At higher velocities (Fig. 6) the scour hole extended alongside the entire pier and a deposition area formed downstream of the pier. The scour pattern of the skewed pier is highly asymmetrical with the maximum scour localized on the side toward which the pier is skewed (Fig. 7). The areas of deposition downstream of the pier were more accentuated. Table 2 summarizes the geometric characteristics of the scour hole in the different runs. It can be noticed that the side slope of the scour hole is steeper for the aligned pier than for the skewed pier.

Contraction Scour

The presence of the pier contracted 7.3% of the channel width at the pier level and 16% at the footing level. The measurements suggest that at least part of the erosion alongside the pier was due to contraction scour. Measured contraction scour depths were

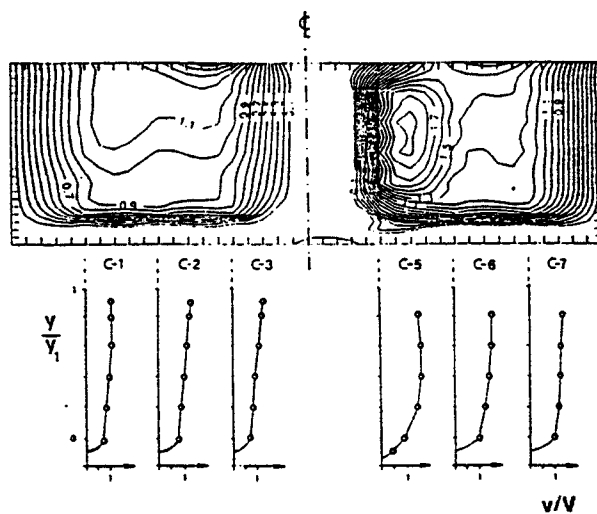


Figure 4. Dimensionless velocity distribution v/V , Run no. 4, sec. C
($V = 0.3$ m/s, $\alpha = 10^\circ$).

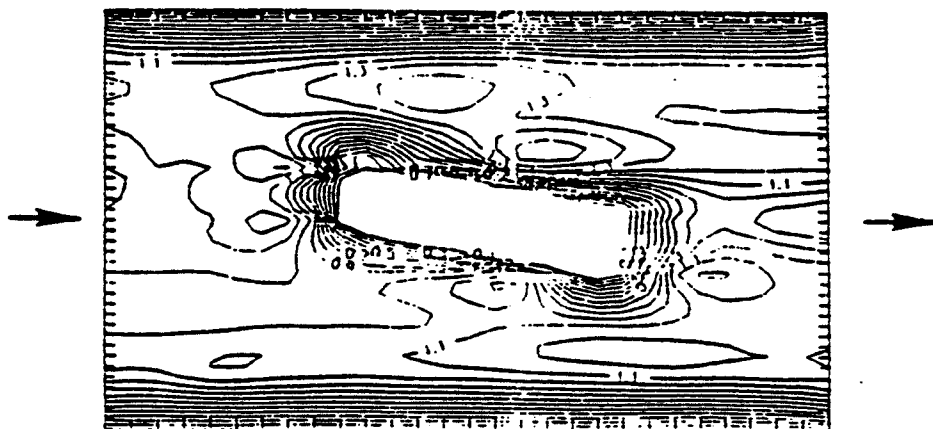


Figure 5. Planview of the dimensionless velocity distribution v/V
at a depth $y = 0.4 y_1$, Run no. 4 ($V = 0.3$ m/s, $\alpha = 10^\circ$).



Figure 6. Scour alongside the aligned pier (Run No. 3).

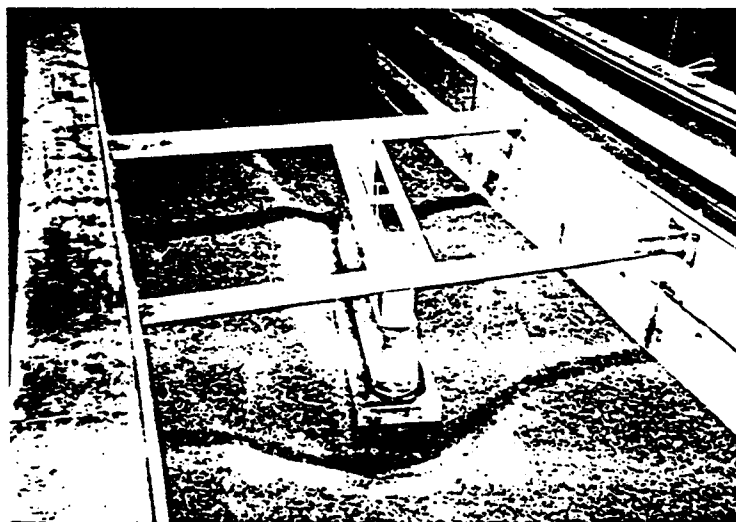


Figure 7. Scour around the skewed pier (Run No. 6).

compared with the depths predicted by Laursen's equation (1980), which computes the contraction scour depth y_c as the difference between the flow depth y_2 in the contracted reach and the upstream flow depth y_1

$$y_c = y_2 - y_1 \quad (1)$$

where y_2 is given by

$$\frac{y_2}{y_1} = \left(\frac{W_1}{W_2} \right)^A \left(\frac{n_2}{n_1} \right)^B \quad (2)$$

in which W is the channel width, n is the Manning's coefficient, A and B are two exponents whose values are tabulated as a function of the mode of transport of the bed material in the contracted reach, and the subscripts 1 and 2, respectively, refer to the undisturbed and contracted reach. Assuming $n_1 = n_2$ while the width ratio is based on the pier width, a constant value of $y_c = 0.035$ m is obtained for all test conditions. This result is compared with the measurements in Figure 8.

Maximum Local Scour Depths

The deepest scour always occurred right in front of the pier where contraction scour is not yet present. This means that the maximum scour depth is not significantly influenced by the contraction scour. It was then possible to compare the measured local scour depths y_{sm} with the maximum calculated scour depth y_{sc} from the following equations:

CSU equation (Richardson et al., 1990):

$$\frac{y_{sc}}{Y_1} = 2.0 \left(\frac{b}{y_1} \right)^{0.65} Fr^{0.43} \quad (3)$$

Laursen (1980) equation:

$$\frac{b}{y_1} = 5.5 \frac{y_{sc}}{y_1} \left[\left(\frac{y_{sc}}{11.5 y_1} + 1 \right)^{7/6} / (\tau_0/\tau_c)^{1/2} - 1 \right] \quad (4)$$

and Froehlich (1987) equation:

$$\frac{y_{sc}}{b} = 0.32 \phi \left(\frac{b'}{b} \right)^{0.62} \left(\frac{y_1}{b} \right)^{0.46} Fr^{0.20} \left(\frac{b}{D_{50}} \right)^{0.08} + 1 \quad (5)$$

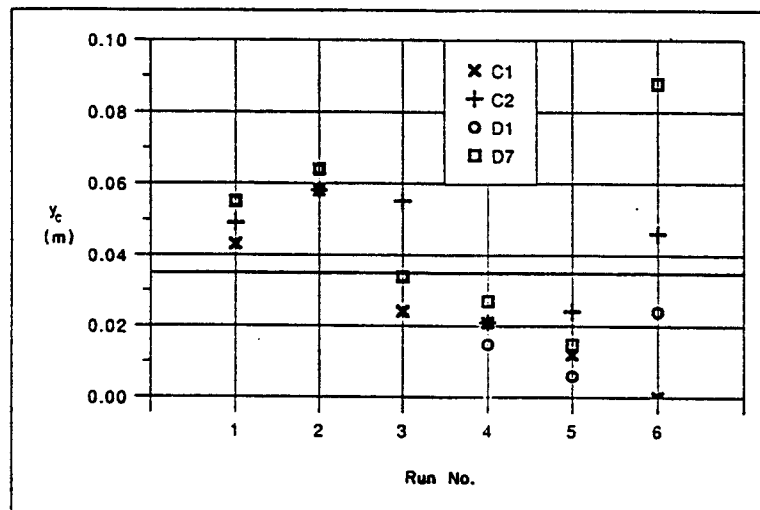


Figure 8. Computed and measured contraction scour depths.

Table 2. Geometric characteristics of the scour hole.

Run number	Upstream flow velocity V [m/s]	Pier angle α	Scour depth y_s [m]	Scour width [m]	Side slope
1	0.3	0°	0.076	0.152	1.00
2	0.6	0°	0.158	0.274	0.87
3	0.9	0°	0.305	0.457	0.75
4	0.3	10°	0.122	0.213	0.88
5	0.6	10°	0.241	0.357	0.75
6	0.9	10°	0.427	0.518	0.61

where, y_1 is the upstream flow depth, b is the pier width, Fr is the Froude number, τ_o is the bed shear stress, τ_c is the critical bed shear stress, b' is the projected pier width normal to the flow direction, D_{50} is the mean sediment size, and ϕ is a pier-shape factor equal to $\phi=1$ for a round-nosed pier.

Since the complex pier geometry provides both the pier width and the footing as possible values for b , calculations of scour depth using both values are considered separately. Figs. 9 and 10 illustrate the results.

It is concluded from our experimental results on Figures 9 and 10 that the pier width, rather than the foundation width, is more appropriate in calculating local pier scour. In general, these equations tend to overestimate the scour depth, with the exception of Laursen's equation which underestimates the scour depth at low Froude numbers.

Influence of the Pier Angle

These experiments allow direct comparison between the scour depth y_{s10° when the pier is angled at 10° , and pier scour of an aligned pier y_{s0° , the other parameters being equal. The ratio $y_s^* = y_{s10^\circ}/y_{s0^\circ}$ between corresponding scour depths separates the effect of the pier angle α in the case of these experiments. Figure 11 compares the values of y_s^* from laboratory measurements obtained from the three scour depth equations. From Fig. 11, a trend is noticed in that the effect of pier orientation seems correlated to the Froude number, decreasing when the Froude number increases. The possibility of a dependence of the angle correction coefficient on the flow velocity (or Froude number) is not unreasonable. First of all, the strength of the vortices depends on both the upstream velocity and the projected pier width perpendicular to the flow direction (which is affected by the pier angle). The influence of the angle of attack might be related to the flow average velocity in the sense that as the Froude number increases (here velocity and Froude number are used interchangeably because the depth remains constant) and the inclination of the pier increases the scour depth cannot increase indefinitely, but must approach an ultimate limit.

Maximum Velocities

Some riprap design methods are based on velocity measurements. Typically, a representative riprap size or stone weight can be determined from average velocity, bottom velocity or a reference velocity. For instance, the Isbash formula relates the riprap stone weight to the sixth power of the velocity. It is then clear that riprap design is highly sensitive to velocity measurements.

In the particular case of riprap design around piers, the velocity increases due to both the contraction effect and the turbulence. Maximum and minimum instantaneous velocities were measured at each point to provide an indication of the maximum velocity fluctuations normally expected around bridge piers. The measurements show that the maximum ratio of the maximum point velocity v_{max} to the average undisturbed velocity V decreases with increasing velocity. The maximum measured ratio is as high as 1.8 and it is registered during Run no. 4.

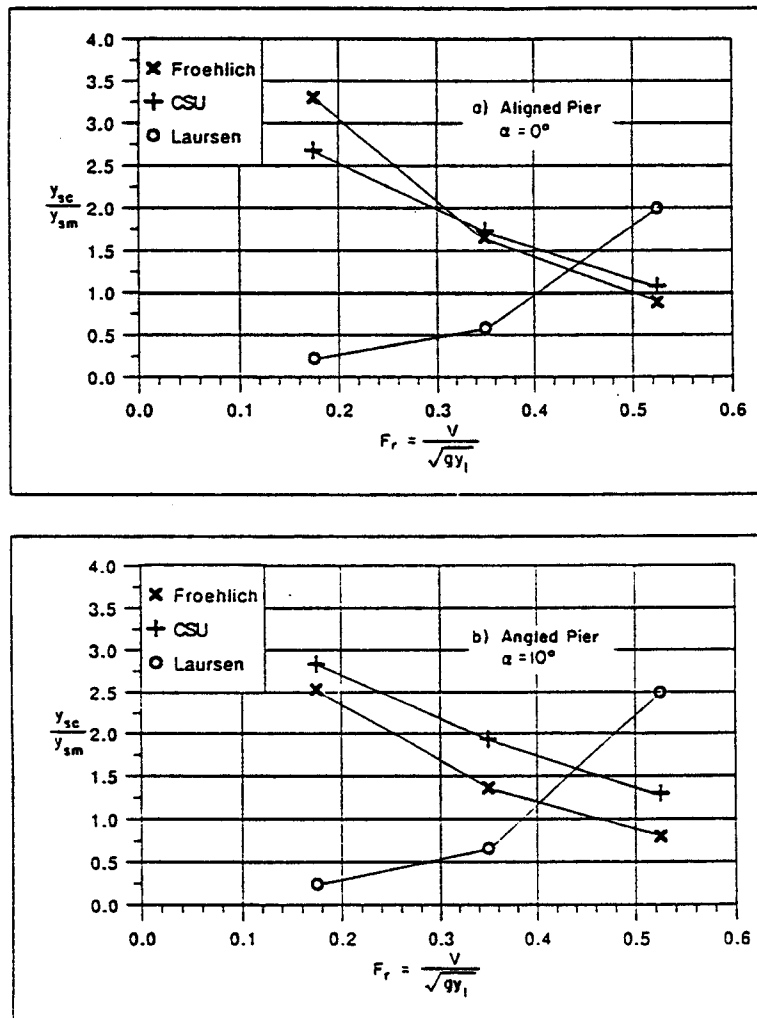


Figure 9. Ratio of computed to measured scour depths using $b =$ pier width.

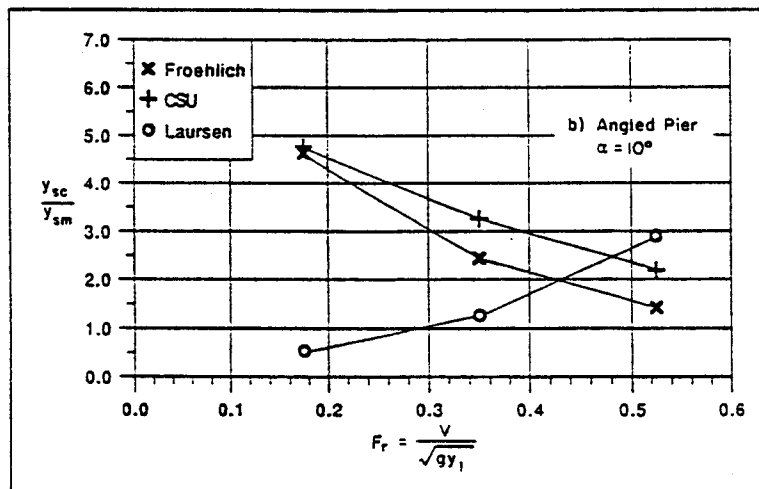
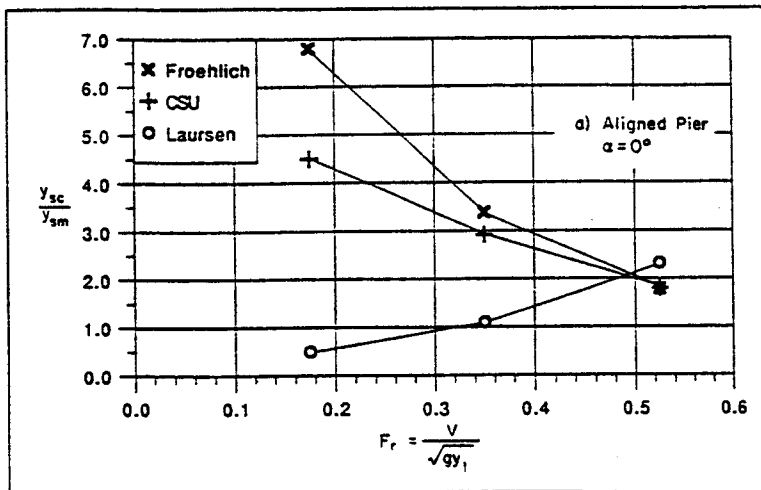


Figure 10. Ratio of computed to measured scour depths using $b =$ footing width.

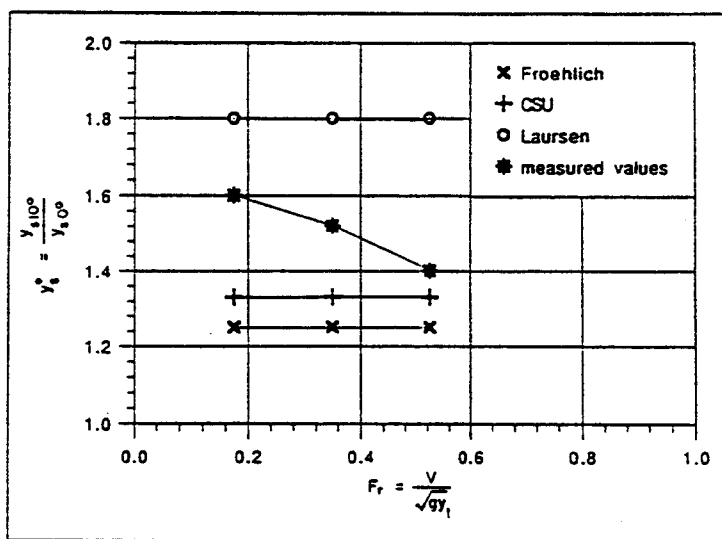


Figure 11. Effect of pier alignment on pier scour.

Possible Armoring Effect

Two samples of the bed material from the surface of the front part of the scour hole were taken and analyzed after the tests. The sieve analyses before and after Run no. 3 indicate that the amount of particles smaller than approximately 2 mm on the scour hole surface had significantly diminished while all the particles smaller than 0.5 mm had been totally washed out. The tests results, however, do not indicate significant armoring effects.

Comparison with Prototype Scour Depth

At a linear scale of 1:15, the Froude number analogy gives a velocity scale 1:3.87. The prototype conditions for which field data were available (Richardson et al., 1988) are closely modeled in Run no. 3. The measured scour depth in the experiments scaled to 4.57 m of scour depth at the prototype scale which compares with the field measured scour depth of 4.27 m.

CONCLUSIONS

The following considerations can be drawn from these laboratory experiments on velocity and scour depth measurements around a model of the Schoharie bridge pier:

1. The time-average point velocity distribution in cross and plan sections shows two areas of increased velocities alongside the pier. The recorded values were as high as 1.6 times the mean upstream approach velocity.
2. With the initial bed surface at the same elevation as the top of the footing, scour depth calculations based on pier width are more appropriate than the footing width.
3. The measured local scour depths are in reasonable agreement with the local scour depths calculated from three scour equations. All equations perform better at higher values of the Froude number ($Fr > 0.3$).
4. The ratio y_s^* of the angled pier scour depth $y_{s(10^\circ)}$ to the aligned pier scour depth $y_{s(0^\circ)}$ decreases with increasing Froude number as shown in Fig. 11. Although few experiments are considered, the detected trend is nevertheless significant.
5. The ratio of the maximum velocity fluctuations to the mean undisturbed upstream velocity decreases as the mean flow velocity increases. Values as high as 1.8 times the mean approach velocity were measured around the angled pier.
6. From the measurements reported at the prototype scale of 1:15, the run with an aligned pier and the maximum velocity (3.48 m/s) gave a scour depth at the prototype scale of 4.57 m which compares with the field measured scour depth of 4.27 m.

APPENDIX I. REFERENCES

- Froehlich, D.C., 1987, "Local Scour at Bridge Piers from Onsite Measurements", U.S. Geological Survey, Water Resources Division.
- Laursen, E.M., 1980, "Predicting Scour at Bridge Piers and Abutments", General Report No. 3, University of Arizona.
- Richardson, E.V., Simons, D. and P.Y. Julien, 1990, "Highways in the River Environment", U.S. Department of Transportation, FHWA-HI-90.016.
- Richardson, E.V., Ruff, J.F. and T.E. Brisbane, 1988, "Schoharie Creek Bridge Model Study", Proceedings of the ASCE, Hydraulic Division Spec. Conference, Colorado Springs, Colorado, August.
- Santoro, V.C., 1989, "Experimental Study on Scour and Velocity Field around Bridge Piers", Thesis in partial fulfillment of the requirements for Master of Science degree, Colorado State University, Fort Collins, Colorado, July.

APPENDIX II. NOTATIONS

b	pier width
b'	projected width of the pier in perpendicular direction to the main flow
D ₅₀	mean sediment size
Fr	Froude number
l	length of the pier
n	Manning roughness coefficient
Q	total discharge
V	mean approach flow velocity
y ₁	upstream flow depth
y ₂	flow depth in the contracted reach
y _c	contraction scour
y _s	maximum depth of scour below mean bed level
y _{sc}	calculated local scour depth
y _{sm}	measured local scour depth
y _{s10°}	scour depth at an angle $\alpha = 10^\circ$
y _{s0°}	scour depth at an angle $\alpha = 0^\circ$
y _s	ratio of y _{s10°} / y _{s0°}
W	width of the channel
α	angle of attack of the flow
ϕ	pier shape factor, $\phi = 1$ for round-nosed piers
τ_o	bed shear stress
τ_c	critical shear stress